JOURNAL OF MATERIALS SCIENCE 28 (1993) 1824–1828

Thermal evolution of Co_{1-x}–P_x electrodeposited ribbons and its influence on the electrical resistivity

F. BRANDA, L. LANOTTE*, A. COSTANTINI
*Dipartimento di Ingegneria dei Materiali e della Produzione, and *Dipartimento di Scienze Fisiche, unità CINFM, Facoltà di Ingegneria, Piazzale Tecchio, 80125 Napoli, Italy*

P. MATTEAZZI
Istituto di Chimica, Facoltà di Ingegneria, via Cotonificio 108, 44133 Udine, Italy

Co–P ribbons have been obtained by electrodeposition on aluminium substrates. The effect of changing the current density (in the range 8–19 A dm^{-2}) and the H_3PO_3 concentration on the nature of the phases present in the "as-prepared" samples and their thermal evolution has been studied by X-ray diffraction analysis and differential scanning calorimetry. Amorphous and crystalline (fully or partly) products have been obtained, by changing the bath composition. Devitrification of the initially amorphous samples leads to cobalt (in the hexagonal and/or cubic form) and cobalt phosphide (Co_2P) crystalline phases. A devitrification mechanism has been proposed. The presence of two amorphous phases in the glassy samples and the possibility of obtaining intermediate samples with crystalline and amorphous phases intermixed with each other, is suggested from the experimental results. The electrical resistivities of the products obtained have been measured. They are affected by the phosphorus content and develop after thermal treatments, in agreement with both microstructure changes and the nature of the crystalline cobalt phases formed.

1. Introduction

The possibility of obtaining amorphous magnetic materials, having low coercive and saturation fields, is of great interest in the production of soft magnets. When produced by casting techniques, metallic glasses require high quenching rates and therefore a splat- or roller-quenching apparatus. Amorphous Co–P alloys are often produced by electrodeposition techniques [1–5] by properly selecting the electrolyte composition and the current density. In this way the phosphorus atomic fraction, x, of the $Co_{1-x}P_x$ alloys can be varied and, when it is higher than 0.11, non-crystalline products are obtained. Correlations between the physical properties and the phosphorus atomic fraction and the alloy structure have been fully established [6, 7]. Usually copper substrates are used, which are asported by means of chemical dissolution (500 g CrO_3 + 50 g H_2SO_4 + 10^3 ml H_2O).

It was shown [8] that amorphous, crystalline and intermediate partly crystalline structures can be obtained by means of electrochemical deposition on an aluminium instead of a copper substrate. In this case, the Co–P deposits can be separated mechanically from the substrate. This property can affect the structural characteristics of the samples because the deposited materials do not form chemical bonds with the aluminium substrate so that new structural characteristics can be obtained as a function of current density [8]. The objective of this investigation was to study both the thermal evolution and the electrical properties of the products obtained by using the non-conventional substrate mentioned above.

2. Experimental procedure

Three bath compositions were used.

(A) 180 g $CoCl_2 \cdot 6H_2O$; 50 g H_3PO_4; 12 g H_3PO_3; 1000 ml H_2O.

(B) 180 g $CoCl_2 \cdot 6H_2O$; 50 g H_3PO_4; 34 g H_3PO_3; 1000 ml H_2O.

(C) 180 g $CoCl_2 \cdot 6H_2O$; 50 g H_3PO_4; 26 g H_3PO_3; 1000 ml H_2O.

A detailed list of the obtained samples is reported in Table I. As can be seen, the current density was changed in the range 8–19 A dm^{-2}. The samples dimensions were fixed by using inert plastic covers (80 $\times$ 3 mm^2) on the aluminium substrate. The last one was accurately lapped and polished. Samples of 72 $\pm$ 10 μm thick were obtained by electrodeposition for times in the range 30–60 min. The samples were subjected to thermal analysis using a Netzsch heat-flux differential scanning calorimeter (DSC) model 404. Al_2O_3 powder was used as reference material. The analysis was performed at a heating rate of 10 °C min^{-1} in a nitrogen atmosphere on small pieces

0022–2461

TABLE I DSC peak temperatures of the electrodeposited samples

Sample	Bath	Current density (A dm^{-2})	DSC peak temperatures (°C)
A_1	A	8.3	–
A_2	A	14.5	–
A_3	A	18.7	–
B_1	B	11.1	296, 372
B_2	B	12.5	282, 389
B_3	B	16.6	243, 404
C_1	C	9.2	449
C_2	C	16.6	455

of Co–P ribbons (~40 mg), suitable for the DSC sample holder, covered with Al_2O_3 powder.

X-ray diffraction analysis was performed using a Siemens diffractometer controlled by an Olivetti M24 personal computer. Using CoK_α radiation, the Co–P samples were examined for an incidence angle within the range 20–80°.

The electrical resistivity measurements were carried out using a potentiostat Solartron 1286 in a galvanostatic four-electrodes configuration. The current intensities across the sample were 10, 10^2 and 10^3 mA.

3. Results and discussion

Fig. 1 shows the DSC curves of the samples. As can be seen, Samples B_1, B_2, B_3, C_1, C_2 all exhibit exothermic peaks when heated in the DSC apparatus. Samples A_1, A_3 (not shown in Fig. 1) behave like sample A_2. It is known that if a glass is heated in a DSC apparatus, when passing through the temperature range of efficient crystal growth (which, in the case of metallic glasses, is usually superimposed on the efficient nucleation temperature range [9]), devitrification takes place and the heat evolved gives rise to an exothermic peak on the DSC curve. Therefore, the DSC results are indicative of the fully crystalline nature of Samples A_1, A_2 and A_3. It is interesting to observe that in the case of Samples B_1, B_2 and B_3 obtained from the Bath B, two exo-peaks were obtained. For the samples from Bath C, only one exo-peak was observed. As can be seen in Table I, the current density during the electrodeposition appears to influence strongly the values of the DSC peak temperature: a difference of 50 °C separates the first DSC peaks of Samples B_1 and B_3.

In order to check the amorphous nature of the other samples and to identify the crystalline phases that they form, after crystallization, X-ray diffraction analysis was performed. Figs 2 and 3 show the XRD patterns of the two sides of the ribbons A_2, B_1, C_2 obtained from the electrodeposition; the "rear" side is that in contact with the substrate. As can be seen, Sample A_2 is confirmed to be fully crystalline. Sample B_1, although somewhat different on the "rear" side, is amorphous. Sample C_2 is only partly amorphous. Therefore, they show substantial differences; minor differences were observed between samples obtained from the same bath. Also taking into account the

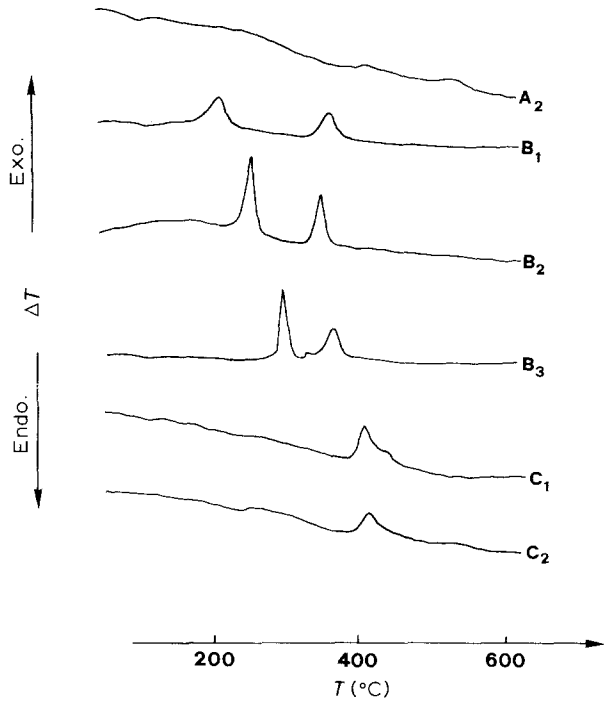

Figure 1 DSC curves of the investigated samples.

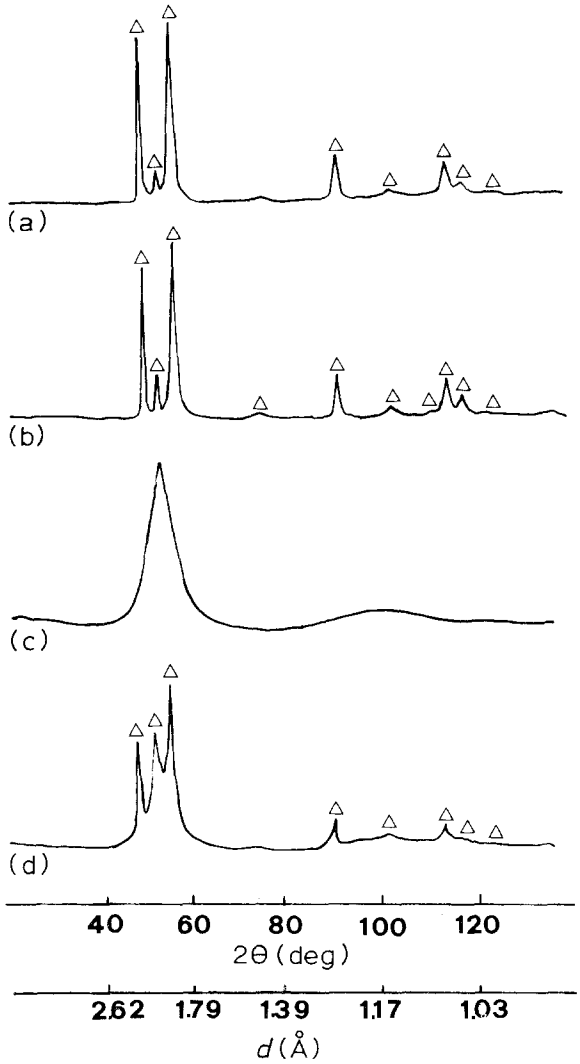

Figure 2 XRD patterns of the samples: (a) A_2 front side; (b) A_2 rear side; (c) B_1 front side; (d) B_1 rear side. (△) Co (JCPDS card 5/727); (□) Co (JCPDS card 15/806); (○) Co_2P (JCPDS card 32/306).

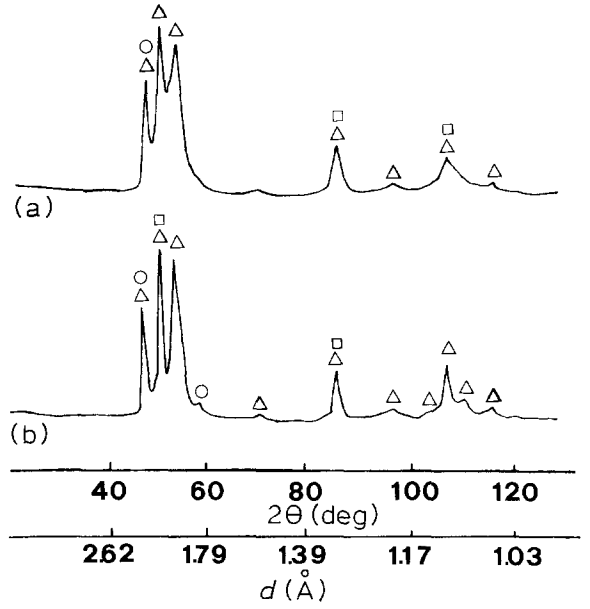

Figure 3 XRD patterns of Sample C_2: (a) front side; (b) rear side. For key, see Fig. 2.

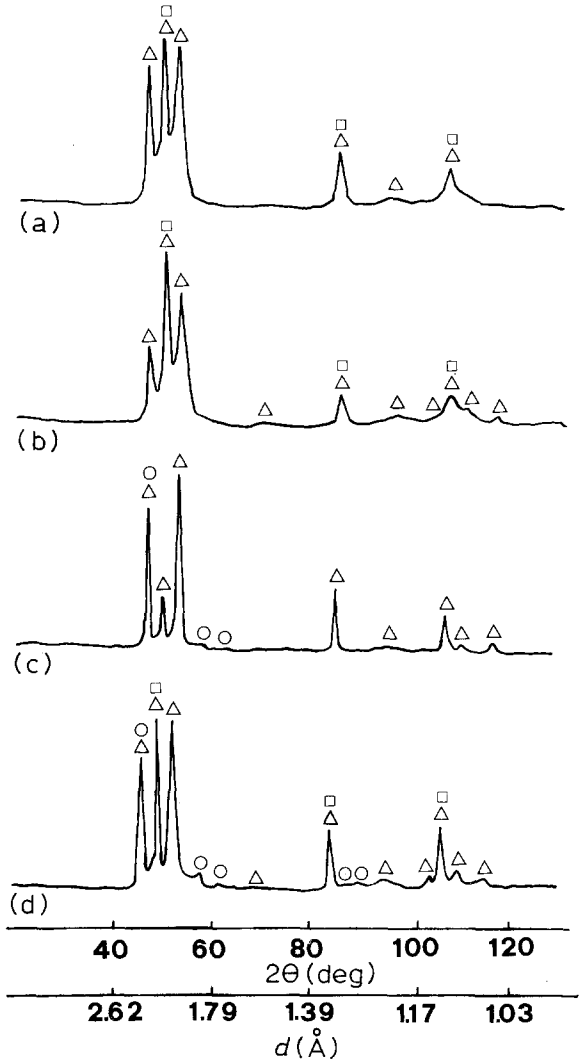

Figure 4 XRD patterns of Sample B_3: (a, b) front and rear sides after 15 min at the first DSC peak temperature, 240 °C; (c, d) front and rear sides after 15 min at 240 °C and 15 min at the second DSC peak temperature, 405 °C. For key, see Fig. 2.

results of Fig. 1, we can therefore distinguish three kinds of sample: those obtained from Bath A which are fully crystalline; those from Bath B, which are predominantly amorphous and give DSC curves with two exo-peaks; and those from Bath C, which are partly amorphous and give DSC curves with only one exo-peak. In the following, therefore, we refer only to Samples A, B and C. Figs 4 and 5 give the XRD results after short heat treatments (15 min), in a nitrogen atmosphere at the temperatures of the exo-peaks of the DSC curves for samples representative of the three types A, B and C. The phases present were identified using JCPDS cards and are indicated in the figures. It is worth remembering that card 15–806 relates to the high-temperature cubic form of cobalt, which is reported to be stable above 450 °C, while JCPDS card 5–727 relates to the low-temperature hexagonal form of cobalt. A martensite start temperature, M_S = 388 °C, is reported on the cards. In Table II, rough values of the crystallization degrees are reported. The superscript primes refer to samples heat treated as specified in the same table. For similar samples, average values are reported; for example, the value attributed to Sample B′ is the average of the values of B_1, B_2 and B_3 heat treated for 15 min at the first DSC peak temperature. They were calculated by evaluating the ratio [10, 11]

$$C\% = \left(1 - \frac{Q_{am}}{Q'_{am}}\right)100 \qquad (1)$$

where Q'_{am} is the integrated intensity of the spectrum of the completely amorphous sample and Q_{am} is the analogous quantity relative to the amorphous halo of the crystallized sample. In the case of C samples it has been assumed that Q'_{am} is the same as for the B samples reported in Fig. 2c.

The XRD results (Figs 4 and 5) confirm that the devitrification process takes place, in B samples, in two steps, coherently with the appearance of two peaks on the DSC curves. These results agree with those reported in the literature [12] for Co–P alloys obtained by electrodeposition under different experimental conditions. The following devitrification mechanism

TABLE II Crystallization degree and electrical resistivities average values. A′, B′ and C′ indicate samples after heat treatment of 15 min at the temperature of the first DSC exo-peak. B″ refers to samples B′ after heat treatments of 15 min at the temperature of the second DSC exo-peak. A′ is a sample of type A annealed for 15 min at 240 °C.

Sample	Crystallization degree (%)		Electrical resistivity
	front	rear	(10^{-5} Ω cm)
A	100	100	6.2
B	0	25	12.1
C	30	65	4.9
A′	100	100	5.7
B′	40	65	7.0
C′	90	90	1.9
B″	80	95	5.3

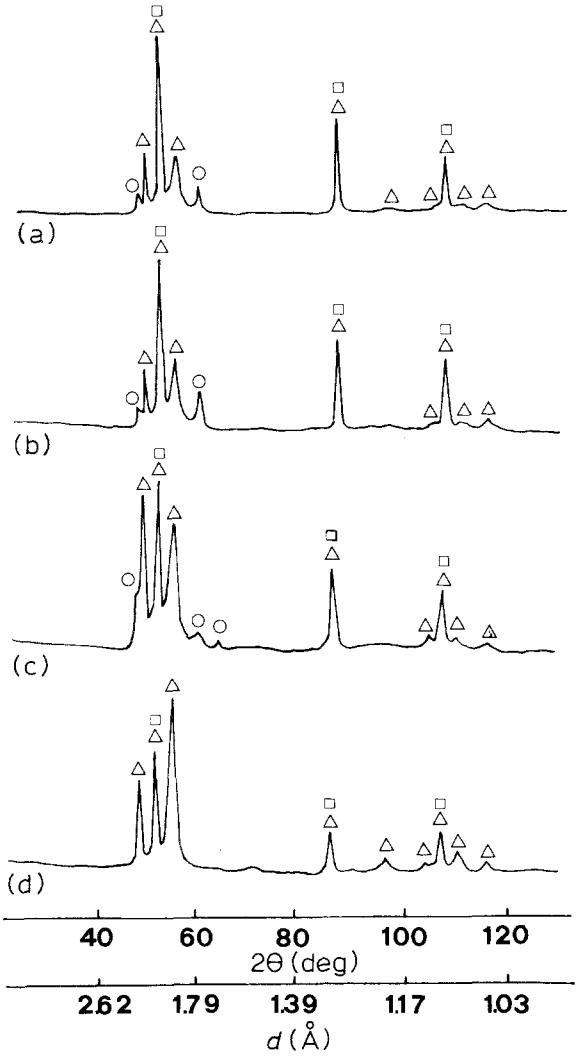

Figure 5 XRD patterns of samples after heat treatments at DSC peak temperatures: (a, b) front and rear sides of C_1 after 15 min at the DSC peak temperature, 450 °C; (c, d) front and rear sides of B_3 after 15 min at the first DSC peak temperature, 280 °C, and 15 min at the second DSC peak temperature, 390 °C. For key, see Fig. 2.

is, therefore, operative in B samples, as already observed [12]

$$a \rightarrow Co + a' \rightarrow Co + Co_2P \qquad (2)$$

where a is the original amorphous phase, a′ is an intermediate amorphous phase.

The C samples, which at origin are only partly amorphous, need only one devitrification step. It is worth noting that they represent a sample type not found in the other work to our knowledge; their formation is, therefore, linked to the nature of the substrate and/or the electrodeposition bath used in the present work. The new structural type of these C samples is related to relevant differences in physical properties, as, for example, already reported for the magnetoelastic coupling [13]. As can be seen in Figs 3 and 5, during devitrification a transformation of the initially present cobalt hexagonal form into the cubic one is also observed, as evinced by the striking change of relative intensity of the three peaks in the range 40–60°. This should be linked to the fact that the heat treatment was performed at the DSC peak temperature of $T = 450$ °C at which the cubic form is reported to be stable. As a consequence, the devitrified A, B and C samples have different crystalline phase compositions. In effect, in A′ the cobalt hexagonal form prevails, whereas in C′, the cubic form is predominant. Fully devitrified B″ samples appear to consist of a mixture of the two phases.

The two-step devitrification mechanism observed in the case of B samples should be linked to the presence of inhomogeneities in the samples. It is known, in fact [14] that, small-angle X-ray and neutron scattering have revealed that the medium-range structure (1–100 nm) in metallic glasses is characterized by compositional inhomogeneities so that metalloid-enriched regions can be distinguished by a metalloid-depleted matrix. The two-stage devitrification can well be the consequence of different devitrification behaviour of the two phases.

In Table II the electrical resistivities of the studied samples are reported. They are average values in the sense indicated above for the crystallinity percentages. It is known that the physical properties are dependent on the phosphorus percentage and the structure of the alloy. It is also known [4, 6–8] that amorphous samples are obtained when $P > 11\%$; moreover, intermediate structures between the fully crystalline and amorphous ones are obtained when $9\% < P < 11\%$. Therefore, the percentage of phosphorus increases in the sequence A, C, B. The results reported in Table II confirm that the structure has a pronounced influence on the properties. In fact, when the crystallinity percentage increases, the electrical resistivity decreases. The electrical resistivity of the fully devitrified B″ samples approaches the values for the fully crystalline A samples, in spite of the different phosphorous percentages. In addition, the nature of the cobalt crystalline phases present appear to have a marked influence. In fact, particularly low values are found in the case of the C "as-prepared" samples, which already contain the cubic cobalt form, and larger values in the fully crystallized samples, C′, in which the cubic cobalt form is the prevailing phase. Also the similarity of electrical resistivity values between the A and B″ samples, in spite of the different phosphorus percentages, could be due to the presence in B″ samples of the cubic cobalt form, which is completely absent in A samples.

4. Conclusions

Crystalline, amorphous and partially amorphous Co–P alloys were obtained by electrodeposition on aluminium substrates (instead of conventional copper ones) by changing the H_3PO_3 concentration in the bath in the range 12–34 $g\,l^{-1}$ H_2O with current densities changing in the range 8–19 $A\,dm^{-2}$. The nature of the phases present in the "as-prepared" samples and their thermal evolution was studied by XRD and DSC. In spite of differences in the DSC peak temperatures, the changes of the current density (in the range studied) do not appear to influence the nature of the phases present in the "as-prepared" samples, and those formed on heating. The H_3PO_3 concentration in the bath is confirmed to determine the amorphous or crystalline nature of the samples. The experimental

results reveal the presence of two amorphous phases in Samples B, while there is only one amorphous phase when disordered and ordered phases are intermixed with each other (C samples). The values of electrical resistivity in the obtained samples appear to change coherently with the differences in microstructure and cobalt crystalline phases.

References

1. R. W. COCHRANE and G. S. CARGILL, *Phys. Rev. Lett.* **32** (1974) 476.
2. D. PAN and D. TURNBULL, *J. Appl. Phys.* **45** (1974) 1406.
3. G. DIEZ and H. DESTGEN, *J. Magn. Magn. Mater.* **19** (1980) 157.
4. K. HULLER and G. DIEZ, *ibid.* **50** (1985) 250.
5. J. M. RIVEIRO, G. RIVEIRO and M. C. SANCHEZ-TRUJILLO, *ibid.* **58** (1986) 235.
6. A. BRENNER, "Electrodeposition of alloys", Vol. 2 (Academic Press, London, New York, 1963) Ch. 35.
7. K. HULLER, M. SYDOW and G. DIEZ *J. Magn. Mater.* **53** (1985) 269.
8. L. LANOTTE, P. MATTEAZZI and V. TAGLIAFERRI, *Mater. Sci. Tech.* **6** (1990)
9. T. KEMÉNY and J. SESTAK. "Comparison of crystallization kinetics determined by isothermal and non-isothermal methods", Budapest 1985.
10. P. H. HERMAN and A. WEIDINGER, *Macromol. Chim.* **44** (1961) 24.
11. A. BENEDETTI, G. COCCO, G. FAGHERAZZI, B. LOCARDI and S. MERIANI, *J. Mater. Sci.* **18** (1983) 1039.
12. K. MASUI, T. YAMADA and Y. HISAMATSU, *J. Jpn Inst. Metals* **44** (1980) 651.
13. L. LANOTTE and C. LUPONIO, *J. Magn. Magn. Mater.* (1991) 2006.
14. P. LAMPARTER and S. STEEB. *J. Non-Cryst. Solids* **106** (1988) 137.

Received 12 November 1991
and accepted 14 August 1992